

## EFFECTS OF Co ADDITIONS ON NANOSTRUCTURE AND MAGNETIC PROPERTIES OF MELT-SPUN $(\text{Nd,Pr})_2(\text{Fe,Ti,C})_{14}\text{B}/\text{Fe}_3\text{B}$ ALLOYS

R. SABBAGHIZADEH<sup>a\*</sup>, M. HASHIM<sup>a</sup>, R. GHOLAMIPOUR<sup>b</sup>, I. ISMAIL<sup>a</sup>, A.OSKOUEIAN<sup>a</sup>

<sup>a</sup>*Advanced Material and Nanotechnology Laboratory, Institute of Advanced Technology (ITMA), Universiti Putra Malaysia, 43400 UPM Serdang, Selangor, Malaysia*

<sup>b</sup>*Advanced Materials and Renewal Energy Dep., Iran Research Organization for Science and Technology (IROST), Tehran, Iran.*

Nanocomposite  $(\text{Nd,Pr})_2\text{Fe}_{14}\text{B}/\text{Fe}_3\text{B}$  magnets were prepared by crystallizing the amorphous melt-spun ribbons. The effects of Co additions on the crystallization behavior, microstructure and magnetic properties of  $\text{Nd}_6\text{Pr}_1\text{Fe}_{76}\text{B}_{12}\text{Ti}_4\text{C}_1\text{Co}_x$  ( $x=0, 3, 6, 9$ ) alloys were studied. As-spun and annealed ribbons were examined by using X-ray diffractometry (XRD), differential scanning calorimetry (DSC) and vibrating sample magnetometry (VSM). The results show that Co additions raise the crystallization temperature. Furthermore, Co substitution promotes the generation of the 2:14:1 phase, which results in a significant increase of coercivity of the ribbons. The proper Co substitution strengthens inter-granular exchange coupling among the grains, and so leads to an obvious enhancement of the remanence and energy product for the  $(\text{Nd,Pr})_2(\text{Fe,Ti,C})_{14}\text{B}/\text{Fe}_3\text{B}$  type ribbons. The best magnetic properties are obtained in the ribbons with  $x = 3$ .

(Received April 12, 2014; Accepted June 11, 2014)

*Keywords:* Nanocomposite magnet; Cobalt; Crystallization; Magnetic properties

### 1. Introduction

Nanocomposite  $\text{Nd}_2\text{Fe}_{14}\text{B}/\text{Fe}_3\text{B}$  melt-spun alloys consisting of a hard magnetic phase exchange coupled to a soft magnetic phase have attracted considerable attention because of their unusually high remanence, high-energy products and low cost [1]. In the  $\text{Nd}_2\text{Fe}_{14}\text{B}/\text{Fe}_3\text{B}$  nanocomposite produced by crystallization of amorphous phase, usually  $\text{Fe}_3\text{B}$  tends to grow during annealing and precipitates sooner than (2:14:1) phase [2]. In nanocomposite magnets the sizes of both the hard and soft phases are in the nanoscale range so that their magnetic moments are exchange coupled. Fischer et al. proposed that an optimum microstructure consists of small soft magnetic grains with sizes of about 10 nm and hard magnetic grains with a mean grain diameter of about 20 nm [3]. If the intergranular exchange coupling is strong enough, the magnetic properties of nanocomposites can be enhanced by optimizing the intrinsic properties of the magnetic phases such as saturation magnetization and anisotropy field [4, 5]. Furthermore, it was found that the size and volume fraction of  $\text{Fe}_3\text{B}$  and  $\text{Nd}_2\text{Fe}_{14}\text{B}$  can be manipulated by thermal processing and by elemental substitution, leading to the increase of the magnetic properties, e.g.,  $B_r$  and  $(BH)_{\text{max}}$ , of the fully processed materials [6]. The most practical method to produce nanostructured metallic materials is rapid solidification. Preparation of a nanocomposite permanent magnet by means of crystallization of a rapidly solidified amorphous alloy involves crystallization of multiple phases. In this article, the influence of Co substitution on the magnetic properties of melt-spun  $\text{Nd}_6\text{Pr}_1\text{Fe}_{76}\text{B}_{12}\text{Ti}_4\text{C}_1\text{Co}_x$  ( $x=0, 3, 6, 9$ ) ribbons is reported. The relationship between the phase component and magnetic properties of the samples has been investigated.

\* Corresponding author: r.h.sabba@googlemail.com

## 2. Experimental procedure

Alloy ingots with nominal compositions of  $\text{Nd}_6\text{Pr}_1\text{Fe}_{76}\text{B}_{12}\text{Ti}_4\text{C}_1\text{Co}_x$  ( $x=0, 3, 6, 9$ ) were prepared from Fe, Nd, and Ti metals with purity greater than 99.5% and commercial-grade Fe–B and Fe–C alloys by induction melting in an argon gas atmosphere and casting onto a chilled hearth. The ingots were remelted four times in order to get the homogeneity. Ribbons were prepared from small pieces of crushed ingots by the single-roller melt-spinning technique at a wheel surface velocity of 25 m/s in an argon gas atmosphere. The chamber Ar pressure was 950 mbar and the ejection pressure was 0.3 bars, and the orifice diameter of the quartz tube was 0.6 mm. The as-spun ribbons were sealed in a quartz tube under  $4.5 \times 10^{-4}$  mbar vacuum and afterwards were isothermally annealed at 640 °C for 10 minutes to optimize their hard magnetic properties then cooled in water. The structure of the ribbons was preliminarily examined using X-ray diffraction (XRD) with monochromatic Cu-K $\alpha$  radiation before and after annealing. Crystallization evolution and determination of crystallization temperature of the as-cast sample was monitored using differential scanning calorimetry (DSC) on SDT 2960 TA Instruments in an Ar atmosphere. Demagnetization curves were measured by using a vibrating sample magnetometer (VSM) after magnetizing the ribbons with a pulsed magnetic field of at least 1.5 T. Field emission scanning electron microscopy (FESEM) micrographs were taken using an FEI NOVANOSEM 230 machine to reveal the microstructure of the sample.

## 3. Results and discussion

Fig. 1 represents X-ray diffraction patterns of as-spun ribbons for different compositions. It shows that the  $x=0$  ribbon, and the ribbons consisting of Co addition have amorphous structures. As mentioned before the wheel speed is constant and because of the straight relation between cooling rate and wheel speed it can be concluded that the cooling rate in our experiment is constant so formation of amorphous structures is due to change of critical cooling rate necessary to form an amorphous structure from the melt. Figure 2 shows the DSC scans for crystallization of all the compositions. For all of them there is only one exothermic peak which means the prior precipitation of  $\text{Fe}_3\text{B}$  was inhibited and crystallization of both  $\text{Fe}_3\text{B}$  and  $\text{Nd}_2\text{Fe}_{14}\text{B}$  occur simultaneously. It is also noticeable that addition of Co increases the crystallization temperature. Besides, these additives narrow the range between the crystallization and transformation temperature. Enhancement of crystallization temperature can be explained by the free volume model [7]. According to this model the amount of free volume necessary for diffusion decreases because of changes in the short range order of local structure of the melt due to Co addition.

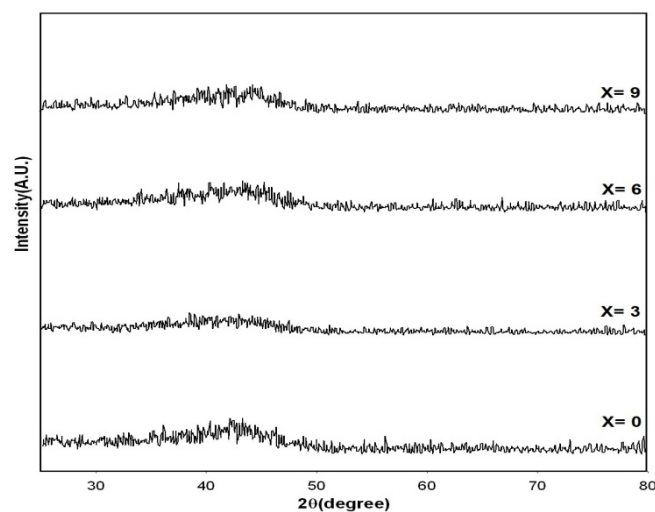


Fig. 1 X-ray diffraction patterns of as-spun ribbons for different compositions.

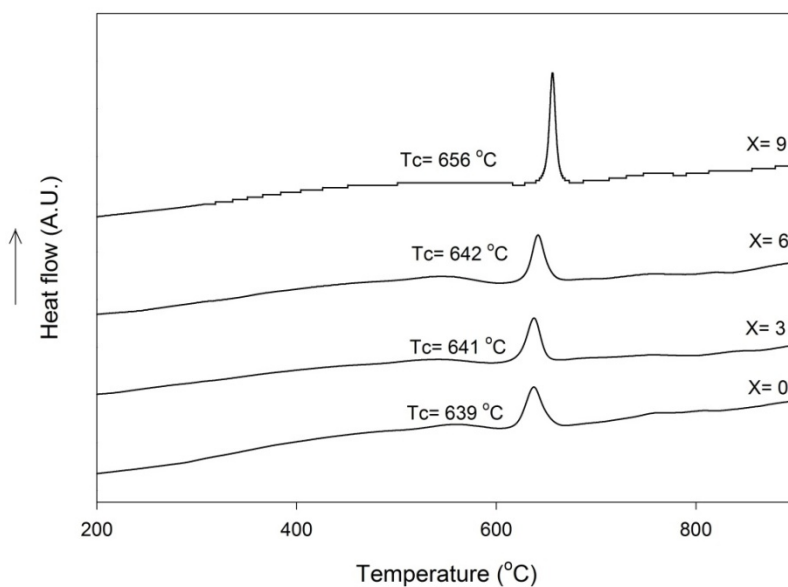


Fig. 2 DSCscans of  $Nd_6Pr_1Fe_{76}B_{12}Ti_4C_x$  ( $x=0, 3, 6, 9$ )

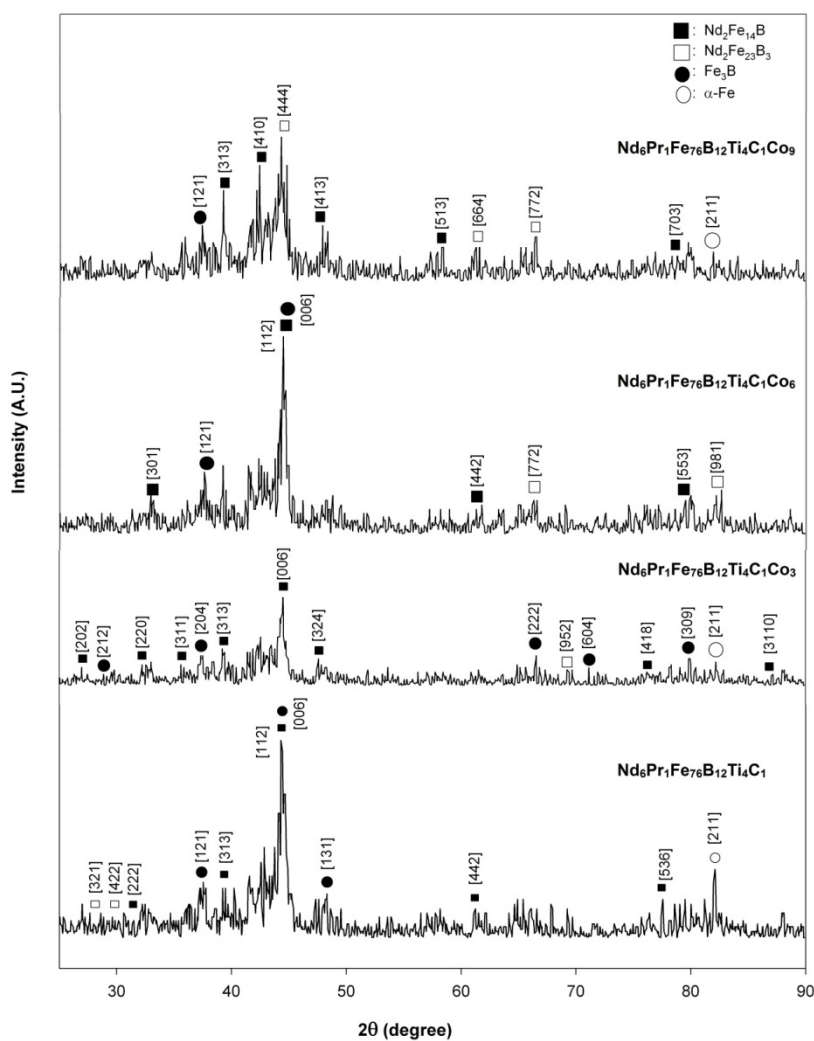


Fig. 3 XRD patterns of ribbons after thermal treatment at  $640^\circ\text{C}$  for 10 minutes.

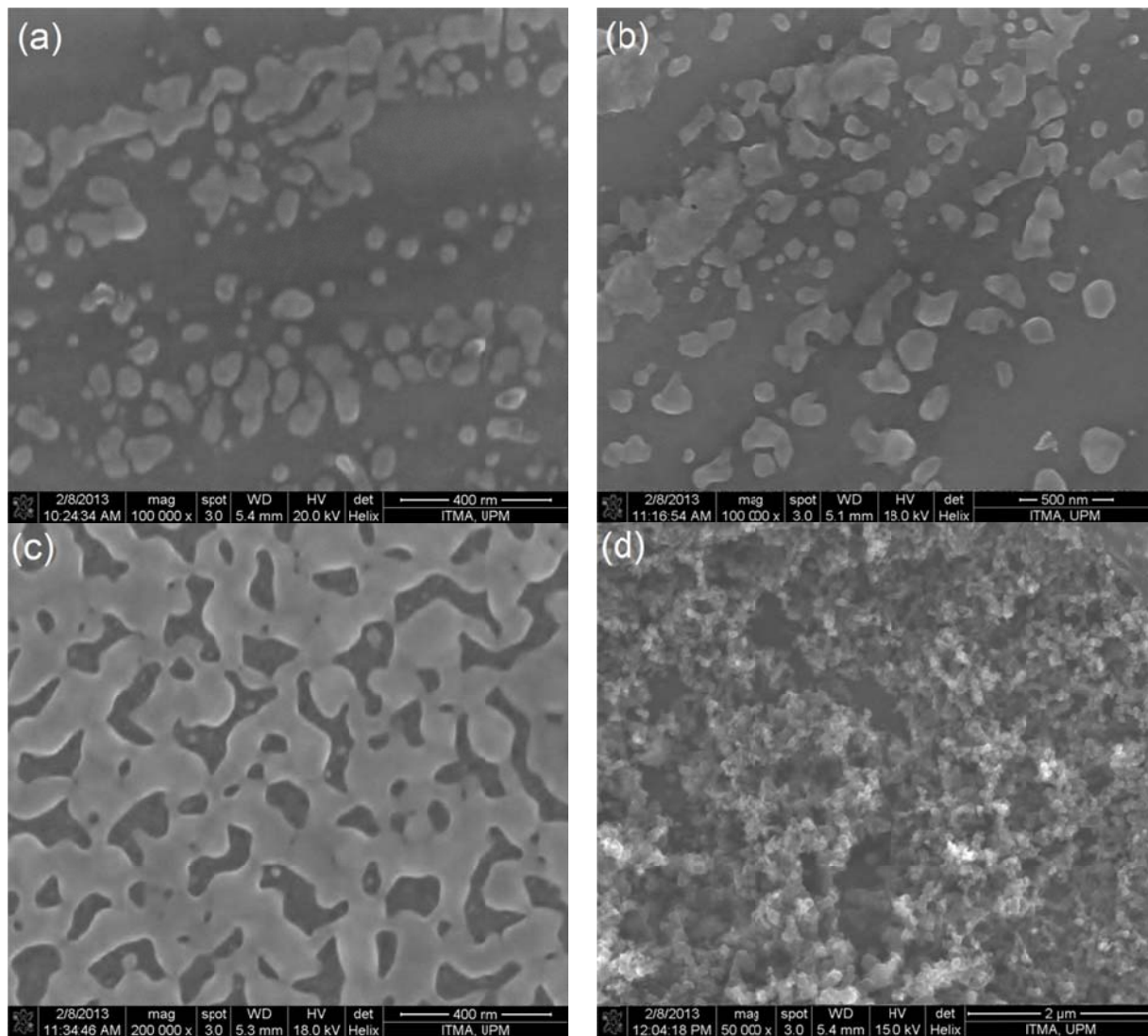


Fig. 4 FESEM morphologies of  $\text{Nd}_6\text{Pr}_1\text{Fe}_{76}\text{B}_{12}\text{Ti}_4\text{C}_1\text{Co}_x$  (a)  $x=0$ , (b)  $x=3$ , (c)  $x=6$ , (d)  $x=9$  Annealed ribbons at  $640^\circ\text{C}$  for 10 minutes.

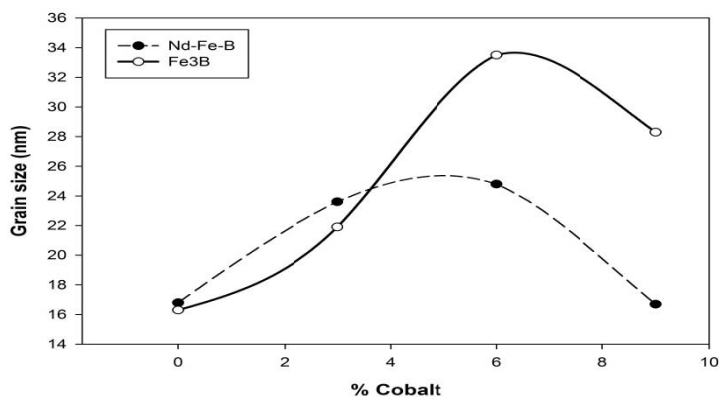


Fig. 5 grain sizes of  $\text{Nd}_6\text{Pr}_1\text{Fe}_{76}\text{B}_{12}\text{Ti}_4\text{C}_1\text{Co}_x$  ( $x=0, 3, 6, 9$ ) annealed ribbons at  $640^\circ\text{C}$  (for 10 minutes) annealing temperature.

Fig. 3 shows powder X-ray diffraction patterns of the annealed ribbons after thermal treatment at  $640^\circ\text{C}$ . It can be seen that the annealed samples consists of  $\text{Fe}_3\text{B}$ ,  $\text{Nd}_2\text{Fe}_{14}\text{B}$ ,  $\text{Nd}_2\text{Fe}_{23}\text{B}_3$  and a trace of  $\alpha\text{-Fe}$ . As can be seen in the diffraction patterns, the formation of the  $\text{Fe}_3\text{B}$  phase is increased with Co increasing up to  $x=3$  and then it decreases. Adding Co can change the

viscosity of the molten metal. Hence, a little increase in the amount of Co could bring the crystallization temperatures of phases closer, leading to uniform grain distribution and improving magnetic properties. Fig 4 shows the surface microstructure of annealed samples. Obviously, the micrographs indicate that grain growth mechanism is occurring. The average grain size of a sintered body was measured over 200 grains by the linear intercept method. The results are shown in Fig 5, the grain size of the  $\text{Fe}_3\text{B}$  and  $\text{Nd}_2\text{Fe}_{14}\text{B}$  crystals are substantially increased by the Co addition, up to 6% (atomic percent) of Co and then decreased. However, it is the 3at% cobalt composition which gives the microstructure with a desired insular morphology for good exchange-coupled magnets, not the 6at%Co composition whose microstructure is beginning to form a continuous polycrystalline phase. According to the DSC curves, the crystallization was terminated at  $640^\circ\text{C}$  for all composition except  $x=9$  whose crystallization occurs a higher temperature of  $656^\circ\text{C}$ . Also, the grain size of the 9at%Co composition is smaller than those of the other compositions. Thus, the grain size and crystallization temperature data above strongly indicate that at 9% Co becomes an inhibitor to crystal growth. Magnetic properties of annealed ribbons were measured by an amplitude gradient force magnetometer (AGFM) with maximum applied field of 1.5 Tesla. The calculated data are summarized in Table 1 which shows that the substitution of Co for Fe significantly improves the magnetic properties of the samples. The remanence ( $B_r$ ) and energy product  $(BH)_{\max}$  first increase with  $x$ , up to the maximum value at  $x=3$ . Further Co substitution results in a decrease of  $B_r$  and  $(BH)_{\max}$  [8]. As can be seen the best magnetic properties are obtained at 3% (atomic percent) of Co addition, which shows the optimum amount of additives. The addition of small amounts of Co, in the nanocomposite permanent alloy enhances all hard magnetic properties. Added Co atoms enter the magnetic hard rhombic (2:14:1) phase, substitute Fe atoms and cause the enhancement of positive exchange interaction and reduction of negative exchange interaction [9]. In addition, the Co atoms can also increase the crystallization temperature of soft phase  $\text{Fe}_3\text{B}$ , and thus enable the grain growth of each phase to be uniform during the crystallization annealing [10]. For the nanocomposite Nd-Fe-B magnet, added Co atoms can substitute Fe atoms of both the hard magnetic phase and the soft phase, yielding  $\text{Nd}_2(\text{Fe},\text{Co})_{14}\text{B}/(\text{Fe},\text{Co})_3\text{B}$  composite magnet, and simultaneously increasing the anisotropy field and the coercivity of the magnet [11].

Table 1 Magnetic properties of  $\text{Nd}_6\text{Pr}_1\text{Fe}_{76}\text{B}_{12}\text{Ti}_4\text{C}_1\text{Co}_x$  ( $x=0, 3, 6, 9$ ) annealed ribbons at  $640^\circ\text{C}$  annealing temperature for 10 minutes.

Composition	Optimum properties at $640^\circ\text{C}$ for 10 min		
	$J_r/J_s$	$H_c$ (KA $\text{m}^{-1}$ )	$(BH)_{\max}$ (KJ/ $\text{m}^3$ )
$\text{Nd}_6\text{Pr}_1\text{Fe}_{76}\text{B}_{12}\text{Ti}_4\text{C}_1$	0.57	216	30.22
$\text{Nd}_6\text{Pr}_1\text{Fe}_{76}\text{B}_{12}\text{Ti}_4\text{C}_1\text{Co}_3$	0.61	223	48.16
$\text{Nd}_6\text{Pr}_1\text{Fe}_{76}\text{B}_{12}\text{Ti}_4\text{C}_1\text{Co}_6$	0.58	215	32.04
$\text{Nd}_6\text{Pr}_1\text{Fe}_{76}\text{B}_{12}\text{Ti}_4\text{C}_1\text{Co}_9$	0.53	203	18.61

#### 4. Conclusion

The relationship between microstructure and magnetic properties of  $\text{Nd}_6\text{Pr}_1\text{Fe}_{76}\text{B}_{12}\text{Ti}_4\text{C}_1\text{Co}_x$  ( $x=0, 3, 6, 9$ ) alloys was interpreted by XRD, DSC and FESEM analysis. In summary, the addition of a little Cobalt in the ternary component (Nd-Fe-B) nanocomposite permanent alloy can increase the crystallization temperature, the anisotropy field and the coercivity [12]. The inter-granular exchange coupling effect is enhanced with the increase of  $x$  ( $x \leq 3$ ). Further increase of  $x$  results in a weaker inter-granular exchange coupling effect. Correspondingly, the  $B_r$  and  $(BH)_{\max}$  of the ribbons first increase with  $x$ , up to a maximum value, and then fall off. However, the best magnetic properties are obtained from the samples which contain 3 at% Cobalt.

### Acknowledgements

The authors would like to thank Mrs Shourchek and Mr Moraddeh for valuable assistance in this research work.

### References

- [1] Z. Wang, W. Liu, B. Zhou, J. Ni, H. Xu, Q. Li, *Rare Metals*, **27**, 299 (2008).
- [2] R. Sabbaghizadeh, M. Hashim, *Electron. Mater.Lett*, **9**, 115 (2013).
- [3] Fischer, R., T. Schrefl, H. Kronmüller, J. Fidler. *Journal of Magnetism and Magnetic Materials* **153**, 35-49 (1996).
- [4] T. Zhao, Q. Xiao, Z. Zhang, M. Dahlgren, R. Grossinger, K. Buschow, F. De Boer, *Applied physics letters*, **75**, 2298 (1999).
- [5] Z. Chen, H. Okumura, G.C. Hadjipanayis, Q. Chen, *Journal of alloys and compounds*, **327**, 201 (2001) .
- [6] I. Betancourt, *Exchange*, **1**, 53 (2009).
- [7] D. Branagan, R. McCallum, *Journal of alloys and compounds*, **230**, 67 (1995).
- [8] Zhang, W. Y., et al. *Journal of alloys and compounds* **379**.1, 28 (2004).
- [9] S.-M. Pan, R.-Z.Ma, G.-B.Li, *Sci. China A* **5**, 538 (1991).
- [10] C.J. Yang, E.B. Park, Y.S. Hwang, *J. Magn.Magn.Mater.***212**, 168 (2000).
- [11] S. Hirose, *J. Appl. Phys.* **73**, 6488 (1993).
- [12] R. Gao, H. Liu, W. Feng, W. Chen, B. Wang, G. Han, P. Zhang, *Materials science & engineering. B, Solid-state materials for advanced technology*, **95**, 187 (2002).